THE ASTROPHYSICAL JOURNAL, 340:666–678, 1989 May 15

THE EVOLUTION OF COOLING FLOWS: SELF-SIMILAR COOLING WAVES

EDMUND BERTSCHINGER[1]
Departments of Astronomy and Physics, University of California, Berkeley, and
Department of Physics, Massachusetts Institute of Technology
Received 1986 July 10; accepted 1988 October 27

ABSTRACT

Similarity solutions are presented for the time-dependent evolution of cooling flows. A cooling flow expands when the cooling time computed from the initial gas distribution increases with radius. If certain simplifying conditions are met, the evolution of the resulting cooling wave becomes self-similar. The similarity solutions obtained here assume subsonic flow, which is valid in the outer parts of observed cooling flows; they are matched to transsonic accretion solutions valid in the central parts. The models are applied to the cooling flow onto M87, with unsatisfactory agreement at small radius. A local linear stability analysis shows that the similarity solution suffers isobaric thermal instability, suggesting that the neglect of star formation may be responsible for the poor agreement. The similarity solution suggests that the cooling flow around M87 was more vigorous in the past.

Subject headings: galaxies: clustering — galaxies: individual (M87) — galaxies: intergalactic medium — galaxies: X-rays — hydrodynamics

I. INTRODUCTION

Hot gas in hydrostatic equilibrium in clusters of galaxies or in galaxy halos cools by the emission of X-rays. Observation of this X-ray emission (Jones and Forman 1984, and references therein) shows that in many cases the gas is sufficiently dense near the center of the potential well to lose most of its thermal energy in less than the age of the system, usually estimated to be $\sim 10^{10}$ yr. In the absence of heating, the cooling gas must move toward the center, initiating a "cooling flow" (Fabian, Nulsen, and Canizares 1984; Sarazin 1986). The cooling gas augments and may even create (Silk 1976) the galaxy onto which it accretes. Thus, cooling flows may present the opportunity for studying galaxy formation in cosmologically nearby objects.

X-ray observations do not directly yield the gas accretion rate or other desired characteristics of a cooling flow; theoretical modeling of the X-ray emission is necessary to derive this information. Ideally, one can derive the gas density and temperature distributions from X-ray imaging and spectroscopic measurements. With the X-ray telescopes flown to date, fairly accurate density profiles have been obtained, but only approximate temperature distributions have been derived, by deprojection of the X-ray surface brightness profile combined with hydrostatic equilibrium and an assumed gravitational mass distribution (Fabian *et al.* 1981). Given the density and temperature profiles and a variety of assumptions, theoretical models can be constructed yielding the mass accretion rate.

Much work has been done on the theoretical modeling of cooling flows, including papers by Fabian and Nulsen (1977), Cowie and Binney (1977), Mathews and Bregman (1978), Cowie, Fabian, and Nulsen (1980), Binney and Cowie (1981), Fabian *et al.* (1981), Takahara and Takahara (1981), Nulsen *et al.* (1982), Tucker and Rosner (1983), Stewart *et al.* (1984), Bertschinger and Meiksin (1986), Silk *et al.* (1986), White and Sarazin (1987), and others. All of the cited work has assumed steady spherical inflow, with various assumptions made regarding energy transport and star formation. Spherical symmetry is probably a good assumption for the best observed cooling flows, except very close to the center (Cowie, Fabian, and Nulsen 1980). The assumption of steady flow, however, while approximately correct close to the center of a cooling flow, is violated in the outer parts. Numerical simulations have provided models of the time-dependent evolution of intracluster gas (Gull and Northover 1975; Lea 1976; Takahara *et al.* 1976; Cowie and Perrenod 1978; Perrenod 1978; Friaca 1986; Bregman and David 1988; Meiksin 1988), and an approximate analytic description of time-dependent cooling has been given by Fabian and Nulsen (1979). However, until the recent work of Chevalier (1987) utilizing self-similarity, no detailed models had been published discussing the role of time dependence on the structure of a cooling flow. The assumptions made by Chevalier concerning initial conditions probably prevent the application of his specific model to real cooling flows. The present paper relaxes these assumptions in order to construct more general time-dependent cooling flow models. A preliminary report of this work was given by Bertschinger (1988).

As a cooling flow evolves, the central region of steady cooling generally expands to encompass an increasing amount of gas. This increase in the size of a cooling flow with time will be denoted a "cooling wave" since, although the region of cooling expands, the gas itself does not move outward. The boundary of the cooling region is set by the cooling radius, i.e., the radius at which the cooling time equals the present age. Because the gas density decreases away from the center (otherwise convective instability would result), the cooling time generally increases outward, and the cooling radius therefore increases with time. At any fixed time, beyond the cooling radius the gas is nearly at rest with the density and temperature profile set by initial conditions, while interior to the cooling radius the gas has begun to cool and flow inward. Far inside of the cooling radius the flow is steady, but near the cooling radius the flow is not steady as each successive element discovers that it must cool and begin a slow fall in to the center. Thus, there are two major consequences of time dependence on cooling flows: the cooling flow expands with time and the

[1] Miller Research Fellow.

structure of the cooling flow changes qualitatively across the cooling radius.

In general, the description of a time-dependent, inhomogeneous flow requires numerical solution of the full partial differential equations of gas dynamics. However, when the time dependence arises through a single physical process (in the present case, cooling), the problem reduces to a self-similar one requiring solution of only ordinary differential equations (Sedov 1959). Although similarity solutions cannot include all of the detailed physics that a realistic time-dependent cooling flow model requires, they do provide valuable insight, are much easier to obtain numerically, and may in some cases provide a satisfactory model. Similarity solutions are thus an appropriate stepping stone from steady models to time-dependent numerical models of cooling flows.

The outline of this paper is as follows. In § II, self-similar cooling waves are derived. The derivation assumes subsonic flow, which is invalid close to the center, where the flow must pass through a sonic point. In § III transsonic accretion solutions with cooling are derived which join on to the similarity solutions between the sonic radius and the cooling radius, yielding a complete description of the cooling flow. The models are applied to the cooling flow onto M87 in § IV. Time dependence of the similarity solution does not solve the problems found earlier by others with steady flows neglecting star formation or heating. A local linear stability analysis shows that the similarity solution is thermally unstable and suggests that star formation may resolve the problems modeling observations. Conclusions are presented in § V.

II. SIMILARITY EQUATIONS AND SOLUTIONS

Cooling wave similarity solutions are derived in this section. Readers not interested in the mathematical details may wish to skip § II*b*.

a) Basic Assumptions

The evolution of a cooling flow will be self-similar, provided that the flow is characterized by a unique scale length, the cooling radius $R_c(t)$. This requires that the gravitational force and the exponential of the specific entropy of the gas be (for $r \gg R_c$) power laws in radius. Equivalently, for $r \gg R_c$, the density and pressure must approach the static solution

$$\rho_0(r) = Ar^{-\alpha}, \quad p_0(r) = Br^{-\beta}, \tag{2.1}$$

where A, B, α, and β are constants. The gas is bound by a gravitating mass distribution

$$M_G(r) = \frac{\beta B}{GA} r^{\alpha-\beta+1}. \tag{2.2}$$

The gravitational potential arises from the galaxy or cluster accreting the gas and is assumed to be static. A singular isothermal mass distribution has $\alpha - \beta = 0$, while a Keplerian distribution has $\alpha - \beta = -1$. For $\beta = 0$, there is no gravity and the cooling gas is confined by the pressure of hot gas at large r. The self-gravity of the gas is neglected. Equation (2.2) is assumed to hold for all r and t.

Equations (2.1) imply that, for $r \gg R_c$, the gas distribution is polytropic with index Γ:

$$p_0 \propto \rho_0^{\Gamma}, \quad \Gamma = \beta/\alpha. \tag{2.3}$$

The polytropic index Γ is determined by events (e.g., cluster collapse and relaxation) occurring before the cooling flow begins. Convective stability requires $0 \leq \Gamma \leq \gamma$, where $\gamma = 5/3$ is the adiabatic exponent of the gas, but Γ is otherwise arbitrary.

The cooling function is assumed to be given by a power law of temperature: $\Lambda \propto T^{\lambda}$. Specifically, the gas cools by optically thin emission at a rate (per unit volume)

$$\mathscr{L} = \rho^2 \Lambda_0 (p/\rho)^{\lambda}, \tag{2.4}$$

where Λ_0 and λ are constants. Thermal bremsstrahlung cooling, which dominates for $T \gtrsim 5 \times 10^7$ K, gives $\lambda = \frac{1}{2}$. At lower temperatures, line cooling dominates, with $\lambda \approx -\frac{1}{2}$ to -1 for a gas of near-cosmic metal abundances (Gaetz and Salpeter 1983). The cooling radius is defined to be the radius at which the cooling time, evaluated *using the static initial gas distribution*, equals the present age t:

$$t_{\rm cool}(R_c) \equiv \frac{p_0(R_c)}{(\gamma - 1)\mathscr{L}(R_c)} = t, \tag{2.5}$$

yielding

$$R_c(t) = [(\gamma - 1)\Lambda_0 A^{2-\lambda} B^{\lambda - 1}]^{\eta} t^{\eta}, \tag{2.6}$$

where

$$\eta = [\alpha + (\alpha - \beta)(1 - \lambda)]^{-1}. \tag{2.7}$$

Thus, the region of cooling expands (for $\eta > 0$) with a power-law dependence on time. For $r \ll R_c(t)$, the cooling time is short compared to t, while, for $r \gg R_c(t)$, the cooling time is long and the gas has not yet cooled appreciably.

The present treatment requires several assumptions in addition to those of power-law forms for the binding mass and entropy profiles and the cooling function. First, spherical symmetry is adopted, which should be a good approximation except close to the center, where angular momentum may become important (Cowie, Fabian, and Nulsen 1980). Second, gas is not removed from the flow (by thermal instability and star formation; see White and Sarazin 1987) for $r > 0$; the only sink for gas is at the center. Likewise, mass input from stars or galaxies (Cowie and Binney 1977) is neglected. The absence of a mass source or sink does not imply constant accretion rate, because the flow is not steady. Third, the cooling wave is assumed to propagate slowly compared to the sound speed at R_c. Finally, heat conduction is neglected, although it may be important for cooling flows (Takahara and Takahara 1981; Tucker and Rosner 1983; Bertschinger and Meiksin 1986; but see Bregman and David 1988) if it is not suppressed by magnetic fields (Stewart *et al.* 1984). The introduction of heat conduction adds a new length scale with a generally different time dependence than the cooling radius, destroying the self-similarity. There is at present considerable uncertainty over the role of heat conduction in cooling flows. Thus, it is useful to construct theoretical models including and neglecting conduction, to attempt to determine observable differences.

b) Fluid Equations and Self-Similarity

The fluid variables must satisfy the usual equations of mass, momentum, and energy conservation:

$$\frac{\partial \rho}{\partial t} + \frac{1}{r^2}\frac{\partial}{\partial r}(r^2 \rho v) = 0, \tag{2.8}$$

$$\frac{\partial v}{\partial t} + v\frac{\partial v}{\partial r} + \frac{1}{\rho}\frac{\partial p}{\partial r} = -\frac{GM_G}{r^2}, \tag{2.9}$$

$$\left(\frac{\partial}{\partial t} + v\frac{\partial}{\partial r}\right)\ln(p\rho^{-\gamma}) = -\frac{(\gamma - 1)}{p}\mathscr{L}. \tag{2.10}$$

To derive similarity solutions, one first defines nondimensional fluid variables by removing the explicit time dependences arising through $R_c(t)$:

$$r = xR_c(t)\,, \quad \rho = \rho_0(R_c)D\,, \qquad p = p_0(R_c)P\,, \quad v = -\frac{dR_c}{dt}\,xW\,. \tag{2.11}$$

The independent variables are transformed from (r, t) to (x, t), and the dependent variables become W, D, and P. The *Ansatz* is now made that, with the explicit time dependences factored out, the dimensional fluid variables are functions of only the dimensionless radius x: $W = W(x)$, and so on. If there are no length scales other than $R_c(t)$, then by dimensionless analysis the time dependence must disappear from the dimensionless fluid variables. In dimensionless form, the fluid equations become

$$(1 + W)\frac{d\ln D}{d\ln x} + \frac{dW}{d\ln x} + 3W + \alpha = 0\,, \tag{2.12}$$

$$\frac{dP}{d\ln x} = -\beta D x^{\alpha-\beta} - \gamma\epsilon D x^2 W\left[(1 + W)\frac{d\ln W}{d\ln x} + W + \frac{1}{\eta}\right], \tag{2.13}$$

$$(1 + W)\frac{d}{d\ln x}\ln(PD^{-\gamma}) = \gamma\alpha - \beta + \frac{1}{\eta}\,D^{2-\lambda}P^{\lambda-1}\,. \tag{2.14}$$

In equation (2.13),

$$\epsilon = \epsilon(t) = \frac{\rho_0(R_c)}{\gamma p_0(R_c)}\left(\frac{dR_c}{dt}\right)^2 \tag{2.15}$$

is the square of the ratio of the propagation speed of the cooling wave to the sound speed in the undisturbed gas at R_c. By assumption, $\epsilon \ll 1$, and the acceleration terms may be neglected in equation (2.13) provided Dx^2W^2 is not large compared with the pressure gradient term. Were this condition to be violated, equation (2.13) would contain (except for special choices of α, β, or λ yielding $\epsilon = \text{const.}$) an explicitly time-dependent term, and the dimensionless fluid variables would necessarily depend on both x and t. When $\epsilon \sim 1$, self-similarity is broken by the presence of two length scales: $R_c(t)$ and $R_s(t) \approx (\gamma p_0/\rho_0)^{1/2}t$. The second length scale corresponds to the outward propagation at the sound speed of a rarefaction wave. If the gas were not already cooling, this wave would signal the gas to begin moving inward, as in the protostellar expansion wave-collapse model of Shu (1977). In the present case the gas is already falling in slowly because cooling decreases the pressure even before the rarefaction wave arrives.

Self-similarity is restored even if $\epsilon \sim 1$, provided that $R_c(t)$ and $R_s(t)$ have the same time dependence so that $\epsilon = \text{constant}$. This is the case considered by Chevalier (1987). The condition $\epsilon = \text{constant}$ imposes the restriction $(3 - 2\lambda)(\alpha - \beta) = 2(1 - \alpha)$ on the parameters of the model. Chevalier considered the case $\alpha = \beta = 1$, an initially isothermal gas distribution with $\rho \propto r^{-1}$. This distribution is too shallow and extended to provide a realistic cooling flow model.

If $\epsilon \neq \text{constant}$, the flow may still be self-similar in a piecewise sense. If the rarefaction wave travels much faster than the cooling wave, i.e., $\epsilon \ll 1$, then the acceleration terms in equation (2.13) will be negligible for $R_c \ll r \ll R_s$. This statement is proven in Appendix A. A necessary and sufficient condition for the validity of this method is given by requiring that ϵ remains small as $t \to \infty$:

$$\beta - \alpha + 2 \le 2/\eta\,. \tag{2.16}$$

If $\epsilon \ll 1$, the acceleration terms are negligible over much of the flow, and equation (2.13) reduces to the equation of hydrostatic equilibrium. The system of equations (2.12)–(2.14) then contains no explicit time dependence and so admits self-similar solutions. The effect of the small time-dependent terms proportional to $\epsilon(t)$ may then be calculated using perturbation techniques. However, this approach breaks down near the two critical points created by the acceleration terms (Chevalier 1987): an outer rarefaction wave and an inner sonic point. The present paper is concerned only with the flow well inside of the rarefaction wave, since typically $R_s \sim 10$ Mpc is much larger than the observed part of a cooling flow atmosphere. In Appendix A it is shown that the rarefaction wave does not significantly disturb the flow for $r \ll R_s$, by showing that the present results agree with those of Chevalier in the case of $\epsilon = \text{constant} \ll 1$.

However, it will be shown below that for any $\epsilon > 0$, the acceleration terms may become large for sufficiently small x, requiring the cooling flow to pass through a sonic point. The self-similarity is therefore broken for $x \ll 1$, and it may appear hopeless to determine the cooling flow evolution without integration of the fully time-dependent equations (2.8)–(2.10). Fortunately, the problem is still tractable using analytic techniques. For $\epsilon \ll 1$, the cooling flow may be divided into two regions: an outer subsonic region, where hydrostatic equilibrium applies and the flow is self-similar, and an inner transsonic region, where the flow is quasi-steady. In § III solutions will be presented for the inner transonic region, and it will be shown how to match these solutions to the similarity solutions for the outer subsonic region. In the remainder of this section, the acceleration terms are neglected in equation (2.13) in order to find similarity solutions valid in the region of subsonic flow.

To integrate equations (2.12)–(2.14), it is helpful to change variables. Define

$$Q \equiv \frac{P}{D}\,x^{\beta-\alpha}\,, \quad E \equiv \frac{1}{\eta}\,Dx^{\alpha-(1/\eta)}\,. \tag{2.17}$$

In these new variables, the dimensionless fluid equations reduce from a third-order system to a second-order system plus a quadrature for $x(W)$:

$$\frac{d\ln Q}{d\ln W} + \frac{d\ln E}{d\ln W} = \frac{G}{F}\left[1 - \eta\beta\left(1 - \frac{1}{Q}\right)\right], \tag{2.18}$$

$$\frac{d\ln Q}{d\ln W} - (\gamma - 1)\frac{d\ln E}{d\ln W} = -\frac{G}{(1 + W)F} \times [\eta E Q^{\lambda-1} + (\gamma - 1)(1 + W) - \eta(\gamma\alpha - \beta)W]\,, \tag{2.19}$$

$$\ln x = -\eta\int^W \frac{G(W')}{F(W')}\frac{dW'}{W'} + \text{const.}\,, \tag{2.20}$$

where

$$F(W) \equiv 1 + [1 + \eta(3 - \alpha)]W\,, \qquad G(W) \equiv W + (1 + W)\frac{d\ln E}{d\ln W}\,. \tag{2.21}$$

Note that a cooling wave similarity solution is specified by four independent dimensionless constants: α, β, γ, and λ. All

numerical examples presented below set $\gamma = 5/3$, appropriate for a monatomic gas.

Outer boundary conditions for the similarity solutions are given by the requirement that as $x \to \infty$ the fluid state must approach the static solution obtained in the absence of cooling, since for $x \gg 1$ the cooling time greatly exceeds the age. Thus,

$$W \to 0\,, \quad Dx^{\alpha} \to 1\,, \quad Px^{\beta} \to 1 \quad \text{as } x \to \infty\,, \tag{2.22}$$

or, in terms of the new variables,

$$Q \to 1\,, \quad E \to 0\,, \quad x \to \infty \quad \text{as } W \to 0\,. \tag{2.23}$$

Inner boundary conditions for the self-similar part of the cooling waves are not as easy to specify, since it is necessary to match the similarity solutions to accretion solutions (§ III). The proper inner boundary condition is that the cooling flow pass smoothly through a sonic point. It will be seen that this condition specifies an eigenvalue problem, where the eigenvalue is essentially the central accretion rate.

Solutions to equations (2.18) and (2.19) have not been found in closed form, so that a numerical solution is necessary. Since it is not possible to start numerical integrations at $W = 0$ ($x = \infty$), a power series solution is desirable for small W:

$$\begin{aligned} Q &= 1 + Q_1 W^{q_1} + Q_2 W^{q_2} + Q_3 W^{q_3} + \cdots\,, \\ E &= E_0 W^{e_0}(1 + E_1 W^{e_1} + E_2 W^{e_2} + \cdots)\,, \\ x &= (\eta E_0 W^{e_0})^{-\eta}\{1 - \eta E_1 W^{e_1} - \eta E_2 W^{e_2} - \eta \\ &\qquad \times [1 - e_0 \eta(3 - \alpha)]W + \cdots\}\,, \end{aligned} \tag{2.24}$$

where $E_0 > 0$, $e_0 > 0$, $e_2 > e_1 > 0$, and $q_3 > q_2 > q_1 > 0$; equations (2.17) and (2.20)–(2.23) have been used. Equations (2.24) implicitly assume $W > 0$, i.e., the gas is flowing inward at infinity. While solutions can be found with $W < 0$, they are probably unphysical. The physical significance of the many possible mathematical solutions to equations (2.18)–(2.23) will be discussed later.

Expressions for the power series exponents and coefficients of equations (2.24) are given in Appendix B, where it is shown that there are two mutually exclusive forms of asymptotic behavior, depending on the values of the parameters α, β, γ, and λ. The first type of solution has $e_0 = 1$ and E_1 (or E_2) arbitrary; all the other constants are determined once E_1 (or E_2) is specified. The second type has $e_0 < 1$ and E_0 arbitrary, with the other constants determined from E_0. It is easily shown that these limiting solutions correspond to subsonic flow as $x \to \infty$ if equation (2.16) is satisfied. For either type of solution, there is one arbitrary constant (E_0, E_1, or E_2) specifying the solution. This freedom exists because inner boundary conditions have not yet been imposed on the solution.

c) *Numerical Solutions*

Figures 1 and 2 demonstrate the effect of varying the eigenvalue E_1 on the solution for the case $\alpha = \beta = 2$, $\lambda = \frac{1}{2}$, corresponding to a singular isothermal sphere binding mass distribution, with constant gas temperature at large radius, and bremsstrahlung cooling. Figure 1 presents density profiles, while Figure 2 graphs the accretion rate as a function of x, where the accretion rate $\dot{m}$ has been nondimensionalized as

$$\dot{m} \equiv -4\pi r^2 \rho v = 4\pi R_c^2\, \rho_0(R_c) \frac{dR_c}{dt}\, \mu(x)\,. \tag{2.25}$$

From equation (2.11) it follows that

$$\mu(x) = x^3 DW\,. \tag{2.26}$$

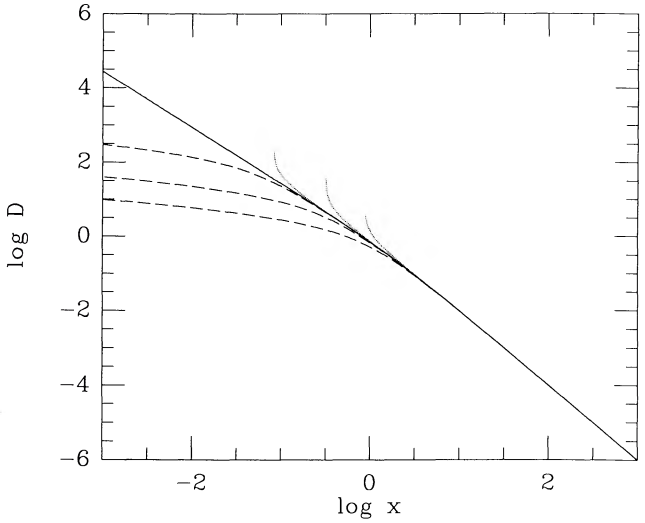

FIG. 1.—Dimensionless density profiles for cooling wave similarity solutions with $\alpha = \beta = 2$, $\lambda = \frac{1}{2}$. All curves satisfy the outer boundary conditions, but only the solid curve (the eigensolution) satisfies the inner boundary condition. The dotted curves have the density diverging at a stagnation point, while the dashed curves have gas flowing in too rapidly for cooling to be important at small radius.

Recall that $\dot{m}$ is constant for a steady flow, and that the similarity solutions are not steady.

As Figures 1 and 2 show, similarity solutions satisfying the outer boundary conditions have three possible types of limiting behavior near the center (see White and Sarazin 1987). The first type of solution is given by the dotted curves. In this case the density becomes infinite, while the pressure remains finite, at some $x = x_0 > 0$. These solutions are similar to the steady cooling flow solutions with stagnation points found by Fabian and Nulsen (1977). In the present case the flow stagnates at a fixed value x_0 (for a given E_1) of the self-similar coordinate, corresponding to a surface moving outward with velocity

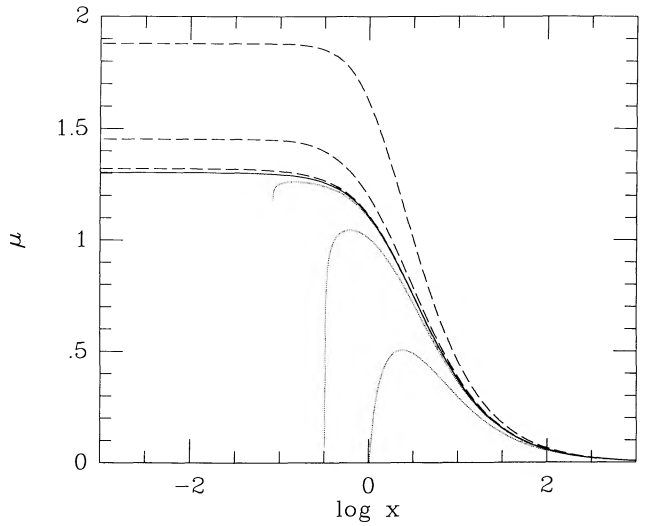

FIG. 2.—Dimensionless accretion rate profiles, corresponding to the density profiles of Fig. 1. The accretion rate is positive for inflow. The dotted curves have outflow close to a stagnation point, which must be driven outward by a piston. The dashed curves correspond to solutions with excessive central accretion rates. Only the solid curve (the eigensolution) passes smoothly through a sonic point at small radius.

$x_0(dR_c/dt)$. The gas settles onto this surface; hence, $W(x_0) = -1$. The inflowing gas comes to a halt and then begins moving outward, so the accretion rate drops to zero, and actually becomes negative, for this type of solution. Solutions of this type are unphysical, since they require a piston moving outward to hold back the inflow. Even if the flow should stagnate because of angular momentum (Cowie, Fabian, and Nulsen 1980) or some other effect (e.g., central heating), there is *a priori* no reason why the stagnation radius should increase with time in the same way as the cooling radius.

The second type of inner solution is illustrated by the dashed curves in Figures 1 and 2. In this case the flow extends all the way to $x = 0$, but cooling becomes unimportant for small x. That is, as $x \to 0$, the flow time

$$t_{\rm flow}(x, t) = r/v = t/(\eta W) \tag{2.27}$$

becomes much less than the cooling time

$$t_{\rm cool}(x, t) = tD^{\lambda-2}P^{1-\lambda} . \tag{2.28}$$

The flow time for $x \ll 1$ is also small compared to the age t, i.e., $W \gg 1$. From the heat equation (2.14), this implies that the specific entropy $\ln(PD^{-\gamma})$ approaches a constant at $x = 0$. The gas flows in too rapidly to cool much at small x. These solutions will be referred to as adiabatic solutions, although it should be noted that cooling does occur at $x \gtrsim 1$.

When the flow time becomes short compared to the age ($W \gg 1$), as occurs at small x in the solutions extending to $x = 0$, the flow becomes quasi-steady. Consequently, the dimensionless accretion rate $\mu \to \mu_0 =$ constant as $x \to 0$ (see eqs. [2.12] and [2.26]). Although the dimensional central accretion rate $\dot{m}(r = 0)$ changes over a time scale t as the cooling wave propagates outward, at small x the gas flows in on a much shorter time scale. This fact allows the similarity solutions to be joined to steady transsonic accretion solutions (§ III).

The solid curve in Figures 1 and 2 shows the third kind of inner behavior for the similarity solutions. This is a unique solution, which will be referred to as the eigensolution, having $t_{\rm flow} \approx t_{\rm cool}$ as $x \to 0$. The eigensolution may be thought of as the limit of the family of solutions with stagnation points as the stagnation radius $x_0 \to 0$. Alternatively, the eigensolution corresponds to the minimum $\dot{m}$ solution of the family of adiabatic solutions. For $\dot{m}$ larger than that of the eigensolution, the gas flows in too quickly to cool, while, for smaller $\dot{m}$, the gas cools completely before reaching the center. It will be shown in § III that the eigensolution is the only solution of the similarity equations satisfying the outer boundary conditions *and* passing smoothly through a sonic point. The eigensolution is therefore the only physically interesting solution for self-similar cooling waves. White and Sarazin (1987) find a similar classification in their steady cooling flow solutions with star formation. However, their model is physically different from the present one—they include star formation and they do not satisfy time-dependent outer boundary conditions—so the agreement in classification of the solutions is not trivial.

It is possible to have mathematical solutions of the similarity equations beginning at $x = 0$ with a smaller central accretion rate μ_0 than the eigensolution. However, integration of the similarity equations shows that such solutions either do not satisfy the outer boundary conditions (eq. [2.23]), or they have outflow as $x \to \infty$. Outflow at large distances can lead to decreased $\dot{m}$ because the gas is first pushed outward before it begins to flow inward. This type of behavior is implausible for astrophysical cooling flows, because there is no obvious mechanism for making the gas flow outward in a self-similar fashion.

It is straightforward to derive the limiting behavior of the eigensolutions for $x \ll 1$. As they must, the results agree with those obtained by Nulsen *et al.* (1982) and Fabian *et al.* (1984) for steady cooling flows. When gravity is unimportant, which is the case if $\beta = 0$ or $\alpha - \beta > 3/(3 - \lambda)$, the density, temperature, and inflow velocity approach power laws in x, with logarithmic slopes

$$\frac{d\ln D}{d\ln x} = -\frac{3}{3-\lambda}, \quad \frac{d\ln(P/D)}{d\ln x} = \frac{3}{3-\lambda}, \quad \frac{d\ln(xW)}{d\ln x} = \frac{2\lambda - 3}{3-\lambda} . \tag{2.29}$$

This case will be referred to as a pressure-dominated cooling wave. Note that the pressure approaches a constant in the center, even though there is a nonvanishing gravitational force, provided $T \gg T_{\rm grav} = (m_{\rm H}/k)(GM_G/r)$. This inequality fails for $\alpha - \beta < 3/(3 - \lambda)$ and $\beta \neq 0$; in this case, denoted gravity-dominated cooling, the power-law exponents become

$$\frac{d\ln D}{d\ln x} = \frac{-3 + (\alpha-\beta)(1-\lambda)}{2}, \quad \frac{d\ln(P/D)}{d\ln x} = \alpha - \beta, \quad \frac{d\ln(xW)}{d\ln x} = \frac{-1 - (\alpha-\beta)(1-\lambda)}{2} . \tag{2.30}$$

Equations (2.29) and (2.30) assume $W \gg 1$, or $t_{\rm flow} \ll t$, for $x \ll 1$. This condition is likely to be satisfied in the central regions of real cooling flows.

The total mass of gas contained within a sphere of radius $r = xR_c(t)$ at time t may be obtained as an integral of the similarity equations. From mass conservation and the continuity equation, it follows that

$$m(r, t) = \frac{4\pi}{3-\alpha}\rho_0(R_c)R_c^3[x^3D(1 + W)] . \tag{2.31}$$

At small x, the quantity in brackets approaches μ_0. Thus, the amount of gas accreted by the central sink is proportional to the total amount of gas interior to the cooling radius. For $\alpha = \beta = 2$, $\lambda = \frac{1}{2}$, numerical integration of the eigensolution gives $\mu_0 = 1.304$. Equations (2.25) and (2.31) also show that the accretion rate is approximately equal to the gas mass enclosed within the cooling radius, divided by the age (Nulsen, Stewart, and Fabian 1984):

$$\frac{t\dot{m}(r=0)}{m(r=R_c)} = \frac{\eta(3-\alpha)\mu_0}{[x^3D(1+W)]_{x=1}} . \tag{2.32}$$

For $\alpha = \beta = 2$, $\lambda = \frac{1}{2}$, the right-hand side equals 0.359.

Equation (2.32) allows a simple estimate of mass accretion rates to be made from X-ray observations of cluster cooling flows, if the assumptions made in deriving the similarity solutions are valid. It should be noted, however, that in the present analysis $R_c(t)$ is defined as the radius where $t_{\rm cool} = t$ from the initial static gas distribution, while observationally one determines the radius where $t_{\rm cool} = t$ from the actual cooling flow. These radii are not very different, and only a small error is made in neglecting the difference between them. Defining x_c such that $t_{\rm cool}(x, t) = t$ (cf. eq. [2.28]), numerical integration gives $x_c = 0.780$ for $\alpha = \beta = 2$, $\lambda = \frac{1}{2}$. If $m(r = R_c)$ is then

TABLE 1

CONSTANTS OF THE SIMILARITY SOLUTIONS[a,b]

α	$\beta = 0.0$	$\beta = 0.5$	$\beta = 1.0$	$\beta = 1.5$	$\beta = 2.0$
			$\lambda = 0.5$		
1.0.....	0.869	1.093	1.738	...	...
	0.555	0.692	0.970	...	...
1.5.....	0.932	1.000	1.149	1.500	2.630
	0.372	0.417	0.486	0.600	0.820
2.0.....	0.965	0.986	1.031	1.119	1.304
	0.232	0.252	0.277	0.310	0.359
2.5.....	0.986	0.990	1.002	1.023	1.063
	0.112	0.120	0.129	0.140	0.153
			$\lambda = 0.0$		
1.0.....	1.200	1.389	1.988	...	...
	0.545	0.703	1.041	...	...
1.5.....	1.095	1.145	1.248	1.500	...
	0.322	0.378	0.460	0.600	...
2.0.....	1.047	1.062	1.091	1.146	1.262
	0.188	0.213	0.244	0.288	0.353
2.5.....	1.018	1.022	1.030	1.042	1.065
	0.087	0.096	0.108	0.122	0.141

[a] For each (α, β, λ), the upper entry gives the dimensionless central accretion rate μ_0; the lower entry gives $t\dot{m}(r = 0)/m(r = R_c)$. See eq. (2.25) and (2.32).

[b] Entries are omitted for solutions which are convectively unstable or violate eq. (2.16).

TABLE 2

CONSTANTS OF THE SIMILARITY SOLUTIONS[a]

α	$\beta = 0.0$	$\beta = 0.5$	$\beta = 1.0$	$\beta = 1.5$	$\beta = 2.0$
			$\lambda = -0.5$		
1.0.....	1.383	1.589	2.250	...	...
	0.493	0.674	1.108	...	...
1.5.....	1.176	1.225	1.310	1.500	...
	0.276	0.337	0.430	0.600	...
2.0.....	1.084	1.100	1.123	1.159	1.225
	0.156	0.182	0.216	0.267	0.347
2.5.....	1.033	1.038	1.044	1.052	1.064
	0.071	0.080	0.092	0.108	0.131
			$\lambda = -1.0$		
1.0.....	1.480	1.714	2.523	...	...
	0.438	0.632	1.169	...	...
1.5.....	1.216	1.267	1.345	1.500	...
	0.239	0.300	0.400	0.600	...
2.0.....	1.103	1.119	1.139	1.163	1.190
	0.133	0.158	0.193	0.248	0.342
2.5.....	1.040	1.045	1.051	1.056	1.061
	0.059	0.068	0.080	0.097	0.122

[a] See notes to Table 1.

replaced by $m(r = x_c R_c)$ in equation (2.32), the right-hand side becomes 0.391, only 9% larger than the value obtained above.

Tables 1 and 2 list, for a grid of parameter values (α, β, λ), the dimensionless central accretion rate μ_0 and the dimensionless ratio $t\dot{m}(r = 0)/m(r = R_c)$, for the cooling wave eigensolutions. The eigensolutions were integrated numerically starting at large x with the series expansions of equations (2.24), varying the coefficient E_0, E_1, or E_2 until the correct inner behavior was realized, as described above. Since the series coefficients have little physical significance, they are not given here.

Tables 1 and 2 show that the dimensionless central accretion rate is usually quite close to $\mu_0 = 1$ for the eigensolution. However, the ratio $t\dot{m}(r = 0)/m(r = R_c)$ can be small for large α and small β. For such cases, the simple estimate of the accretion rate, $\dot{m} \approx m(r = R_c)/t$, leads to a large overestimate. The reason is that, for large α and small β, $\eta(3 - \alpha) \ll 1$, and the mass enclosed by the cooling wave increases much more slowly than $m(r = R_c)/t$. Thus, a better estimate of the central accretion rate is given by

$$\dot{m}(r = 0) \approx \frac{d}{dt}\, m(r = R_c) = \eta(3 - \alpha)\, \frac{m(r = R_c)}{t}\,. \quad (2.33)$$

Equation (2.33) leads to an underestimate of the accretion rate. However, the resulting $\dot{m}$ will be approximately correct if multiplied by (1.80, 1.50, 1.33, 1.15) for $\alpha = (1.0, 1.5, 2.0, 2.5)$; this coefficient has a weak dependence on β and λ.

III. TRANSSONIC ACCRETION WITH COOLING

Section II presented similarity solutions for cooling waves, under the assumption of subsonic flow. This assumption was shown to be valid outside of and somewhat interior to the cooling radius $R_c(t)$ if the cooling wave propagates slowly compared to the sound speed at R_c ($\epsilon \ll 1$; see eq. [2.15]) and if equation (2.16) is satisfied. However, for $r \ll R_c(t)$ the Mach number may increase toward the center, and the assumption of subsonic flow may be violated. The similarity solutions give the square of the Mach number as

$$f \equiv \frac{\rho v^2}{\gamma p} = \frac{\epsilon x^2 W^2}{\theta}\,, \quad (3.1)$$

where $\theta \equiv P/D$ is the dimensionless temperature. From equations (2.26), (2.29), and (2.30), it is easily shown that f for the eigensolution increases without limit as $x \to 0$ if $\lambda < 9/4$ for pressure-dominated cooling, or if $(\alpha - \beta)(2 - \lambda) > -1$ for gravity-dominated cooling. Although it is possible that $f \to 0$ as $x \to 0$ (e.g., $\alpha = 2$, $\beta = 3$, $\lambda = \frac{3}{4}$), such cases are not expected to arise in practice. Thus, the similarity solutions break down sufficiently close to the center, where transsonic accretion solutions with cooling must be found.

For small x the self-similar flow becomes quasi-steady, since the gas flows in on a time scale much less than the age ($t_{\rm flow} \ll t$ or $W \gg 1$; see eq. [2.27]). This fact allows the cooling wave similarity solutions to be matched to steady transsonic flow solutions. Consider the nondimensional fluid equations (2.12)–(2.14). In the equation of motion (2.13), the acceleration terms ($\propto \epsilon \ll 1$) were neglected in deriving the similarity solutions; their inclusion would have led to an explicit time dependence [since $\epsilon = \epsilon(t)$], violating self-similarity. It was shown in § II*b* that the acceleration terms can be ignored outside of and somewhat interior to the cooling radius. These terms cannot be neglected in the vicinity of the sonic point, where $f = 1$. However, for $\epsilon \ll 1$ the sonic point occurs at $x = x_* \ll 1$, where $t_{\rm flow} \ll t$; then, since ϵ changes on a time scale much longer than the flow time, it may be treated as a constant in equation (2.13). If $W \gg 1$ a further simplification occurs, since the accretion rate approaches a constant ($\mu = \mu_0$), eliminating the continuity equation. Thus, for $x \ll 1$ the nondimensional fluid equations become

$$x^3 DW = \mu_0\,, \quad (3.2)$$

$$\gamma f \frac{d}{d\ln x} \ln(xW) + \frac{d\ln P}{d\ln x} = -\frac{\beta x^{\alpha-\beta}}{\theta} \equiv -\phi\,, \quad (3.3)$$

$$\frac{d}{d\ln x} \ln(PD^{-\gamma}) = \frac{D\theta^{\lambda-1}}{\eta W}\,. \quad (3.4)$$

Solutions to these equations are sought which match on to the similarity solutions for $f \ll 1$ and $W \gg 1$, and which pass smoothly through a sonic point $f = 1$ at $x = x_*$. It should be noted that, although they are written in nondimensional form, equations (3.2)–(3.4) are equivalent to the steady ($\partial/\partial t = 0$) fluid equations (2.8)–(2.10), and therefore the transsonic cooling accretion solutions presented below find application in contexts other than cooling waves.

Mathews and Bregman (1978) also considered transsonic accretion with cooling. Their equations (2.1)–(2.3) are equivalent to equations (3.2)–(3.4). Their work differs from the present work in that they assumed the flow to be steady everywhere, but they used more realistic forms of the gravitational mass distribution $M_G(r)$ and cooling function $\Lambda(T)$. The present treatment includes the nonsteady (self-similar) behavior near the cooling radius, but requires power-law approximations for $M_G(r)$ and $\Lambda(T)$ (see eqs. [2.2] and [2.4]).

Before transsonic flow solutions to equations (3.2)–(3.4) are given, it is necessary to show that such solutions exist only for the eigensolutions. In § II*c* (see Figs. 1 and 2) it was shown that there are two classes of solutions to the similarity equations satisfying the outer boundary conditions and extending to small x: a family of adiabatic solutions and a unique (for given α, β, γ, and λ) eigensolution. (The third type of solution found in § II requires the cooling flow to be pushed outward by a piston and is unphysical.) The adiabatic similarity solutions have the specific entropy approaching a constant at small x, or

$$S \equiv PD^{-\gamma} \rightarrow \text{constant} \quad \text{as } x \rightarrow 0 . \tag{3.5}$$

In this case the equation of motion may be integrated to give (for $\alpha \neq \beta$; see Bondi 1952)

$$\frac{1}{2}\gamma\epsilon x^2 W^2 + \frac{\gamma}{\gamma - 1}\frac{P}{D} + \left(\frac{\beta}{\alpha - \beta}\right)x^{\alpha - \beta} = \text{constant} . \tag{3.6}$$

To demonstrate that there is no solution passing smoothly through a sonic point, assume the contrary. Then, for $f \gg 1$ ($x \ll x_*$), the first term of equation (3.6) dominates the second term, while, for $f \ll 1$ ($x \gg x_*$), the reverse is true. For $\alpha > \beta$ and $x \ll 1$, it is straightforward to show that for $f \ll 1$ (subsonic region), $f \propto x^{-4}$, while, for $f \gg 1$ (supersonic region) $f \propto x^{2(\gamma - 1)}$. The solution $f(x)$ therefore does not extend to $x \ll x_*$ and is double-valued for larger x, which is impossible for a fluid. Similar results obtain for $\alpha < \beta$ and $\alpha = \beta$. Thus, the assumption that the adiabatic solutions pass smoothly through a sonic point is incorrect. Either the flow must be nonsteady, or a shock transition from a supersonic to a subsonic branch of the solution must occur. Intuitively, one expects such a flow to be nonsteady, with the central accretion rate dropping because the pressure is too high, until the gas can cool as quickly as it flows in and the eigensolution is obtained. Numerical hydrodynamical simulations would be helpful in studying this type of evolution.

For the eigensolution, the specific entropy is not constant, but decreases due to cooling as $x \rightarrow 0$. Unfortunately, in this case the fluid equations (3.3) and (3.4) can no longer be integrated analytically, but must be solved numerically. For this, it is convenient to recast the equations in a slightly different form. First, normalize the radius and the exponential of the specific entropy to their values at the sonic radius:

$$\xi \equiv \frac{x}{x_*} , \quad \Sigma \equiv \frac{PD^{-\gamma}}{S_*} , \tag{3.7}$$

where x_* and S_* depend on ϵ and are to be determined. After some algebra, the fluid equations become

$$\frac{d\ln\Sigma}{d\ln\xi} = \Sigma'_* \xi^{4a-1} f^{a-1} \Sigma^{-b} , \tag{3.8}$$

$$(f - 1)\frac{d\ln f}{d\ln\xi} = 4 + 2(\gamma - 1)f - \frac{(\gamma f + 1)}{\gamma}\frac{d\ln\Sigma}{d\ln\xi} - \frac{(\gamma + 1)}{\gamma}\phi , \tag{3.9}$$

$$\phi = \phi_* \xi^{4c+\alpha-\beta} f^c \Sigma^{c-1} , \tag{3.10}$$

where

$$\Sigma'_* \equiv \left(\frac{\mu_0}{\eta\epsilon^{1-\lambda}}\right)\left(\frac{S_*\mu_0^{\gamma-1}}{\epsilon}\right)^{-b} x_*^{4a-1} ,$$
$$\phi_* \equiv \left(\frac{\beta}{\epsilon}\right)\left(\frac{S_*\mu_0^{\gamma-1}}{\epsilon}\right)^{c-1} x_*^{4c+\alpha-\beta} , \tag{3.11}$$

and

$$a \equiv \left(\frac{\gamma - 1}{\gamma + 1}\right)(2 - \lambda) , \quad b \equiv \frac{2(2 - \lambda)}{\gamma + 1} , \quad c\left(\frac{\gamma - 1}{\gamma + 1}\right) . \tag{3.12}$$

It is not possible to integrate numerically through the sonic point, so one must begin integrations at the sonic point with a series expansion:

$$\Sigma = 1 + \Sigma'_*(\xi - 1) , \quad f = 1 + f'_*(\xi - 1) , \quad |\xi - 1| \ll 1 . \tag{3.13}$$

Requiring f'_* to be finite yields

$$\Sigma'_* = 2\gamma - \phi_* . \tag{3.14}$$

In addition, one obtains a quadratic equation for f'_*:

$$f'^2_* - 2Af'_* - B = 0 , \tag{3.15}$$

where

$$A = \left(\frac{\Sigma'_*}{2\gamma}\right)[\gamma - (\gamma - 1)(2 - \lambda)] ,$$
$$B = \left(\frac{\gamma + 1}{\gamma}\right)\{\Sigma'_*(b\Sigma'_* - 4a + 1) - (\gamma + 1)\phi_* \times [(c - 1)\Sigma'_* + 4c + \alpha - \beta]\} . \tag{3.16}$$

As is usual in transsonic flow problems, there are two solutions passing through the sonic point. One root, $f'_* = A + (A^2 + B)^{1/2} > 0$, corresponds to a cooling, outflowing wind. The other root, $f'_* = A - (A^2 + B)^{1/2} < 0$, corresponds to the desired transsonic cooling accretion solution.

To integrate equations (3.8) and (3.9), one must first specify ϕ_*, the ratio of the "gravitational" temperature to the gas temperature at the sonic radius. In the case of pressure-dominated cooling (see eq. [2.29]), $T \gg T_{\rm grav}$ for $x \ll 1$, and thus $\phi \ll 1$ throughout the entire steady accretion region. In this case of gravity-dominated cooling (see eq. [2.30]), however, $\phi \sim 1$ for $x \ll 1$. Now ϕ_* is an eigenvalue of the transsonic solution which is determined by requiring that the solutions match onto the cooling wave similarity solutions for $\xi \gg 1$ and $x \ll 1$.

Figure 3 illustrates the transsonic accretion solution for the gravity-dominated cooling case $\alpha = \beta = 2$, $\lambda = \frac{1}{2}$, for which $\phi_* = 2.013$. Other cases are qualitatively similar. Several features are worth noting. First, moving outward from the sonic

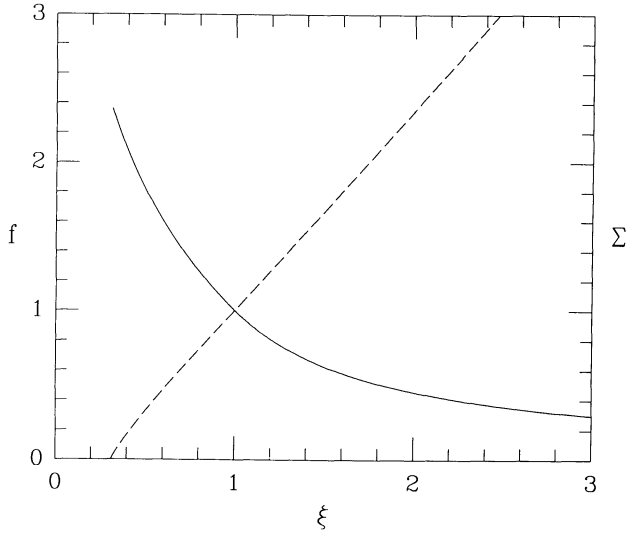

FIG. 3.—Transsonic cooling accretion solution for $\alpha = \beta = 2$, $\lambda = \frac{1}{2}$. The Mach number squared f (*solid curve*) and the exponential of the specific entropy Σ (*dashed curve*) are plotted on the same scale against the radius in units of the sonic radius.

radius $\xi = 1$, the Mach number ($=f^{1/2}$) decreases and the specific entropy of the gas ($\propto \ln \Sigma$) increases. This is as expected: as the gas flows in it cools and accelerates. The surprising result is that the gas cools completely before reaching the center—in the present case, $\Sigma = 0$ at $\xi = 0.313$. This behavior occurs because the power-law cooling allows a thermal runaway. A similar effect occurs behind radiative shock waves (Chevalier and Imamura 1982; Bertschinger 1986). As in the case of radiative shocks, thermal instabilities may be expected to occur here. Thus one should not expect the theoretical solution to model accurately real cooling flows interior to the sonic radius, where the flow is likely to be complicated because of thermal instabilities, repressurizing shocks, star formation, and so on.

Given the accretion solution in the form $f(\xi)$, $\Sigma(\xi)$, it is straightforward to determine the fluid variables. The dimensionless temperature follows from equations (3.3) and (3.10):

$$\theta = \frac{P}{D} = \epsilon\left(\frac{S_* \mu_0^{\gamma-1}}{\epsilon}\right)^{1-c} (x_* \xi)^{-4c} f^{-c} \Sigma^{1-c} . \qquad (3.17)$$

The velocity xW now follows from equation (3.1), and the density D from equation (3.2). It is found that, as expected, at large ξ the fluid variables have the same power-law dependences on ξ as the self-similar eigenfunctions have on $x = \xi x_*$ for small x. Thus, the steady accretion solutions may be joined to the similarity solutions. To accomplish the matching, one requires expressions for the sonic radius x_* and the entropy normalization constant S_* in terms of the parameter ϵ. Extrapolating the similarity solution (eqs. [2.29] and [2.30]) all the way in to the sonic radius and using equation (3.1) yields a proportionality between ϵ and a power of x_*:

$$\epsilon = \begin{cases} K x_*^{(9-4\lambda)/(3-\lambda)}, & \text{pressure-dominated cooling;} \\ K x_*^{1+(\alpha-\beta)(2-\lambda)}, & \text{gravity-dominated cooling.} \end{cases} \qquad (3.18)$$

The constant of proportionality K is determined by actually matching the fluid variables of the steady and self-similar solutions. Once x_* is determined, S_* follows from Σ'_* and μ_0 through equations (3.11) and (3.14). For the case $\alpha = \beta = 2$, $\lambda = \frac{1}{2}$, one obtains $K = 0.501$. It does not matter exactly where the matching is done, provided $\xi \gg 1$ and $x \ll 1$. Of course, this requires $x_* \ll 1$, and hence $\epsilon \ll 1$. If ϵ is not small, the sonic radius is not far inside of the cooling radius, and the flow cannot be divided into regions of self-similar and steady flow. It is interesting that the properties of the cooling flow at $r = R_c$ determine the location of the sonic radius.

Figure 4 presents the complete dimensionless density and temperature profiles for the steady accretion and self-similar cooling wave solutions, for the standard case $\alpha = \beta = 2$, $\lambda = \frac{1}{2}$. The parameter ϵ has been set to 5×10^{-6}, corresponding to a sonic radius $x_* = 10^{-5}$. The matching has been performed at $x = 1.5 \times 10^{-3}$, but because of the large region of overlap of the two solutions, the matching point could have been selected anywhere in the interval $10^{-3.5} \lesssim x \lesssim 10^{-1.5}$. For $x \gg 1$ the fluid approaches its unperturbed state, with $D = x^{-2}$ and $\theta = 1$; because of the low density the gas has not had time to cool appreciably. As the gas flows through the cooling radius $x = 1$ (more precisely, as the cooling wave reaches an initially static gas element), cooling becomes important. Paradoxically, the temperature increases because as the gas cools, it begins to flow inward, and is therefore compressed and heated adiabatically. The time scales for cooling ($t_{\rm cool}$) and compression ($t_{\rm flow}$) are similar, so it is not unreasonable that the temperature increases somewhat. As the gas passes through the cooling radius, the density profile bends over to $D \propto x^{-3/2}$. Interior to the cooling radius there is a large range in radius where the flow is steady and subsonic, but as the gas flows in, its velocity increases ($v \propto x^{-1/2}$), and eventually the flow becomes supersonic. Interior to the sonic point the temperature drops rapidly and the density becomes large. For smaller ϵ (e.g., at later times) Figure 4 would look the same except that the region of steady, subsonic flow would be more extended.

IV. APPLICATION TO M87

In this section the cooling wave solutions developed in §§ II and III are applied to the cooling flow onto the giant elliptical

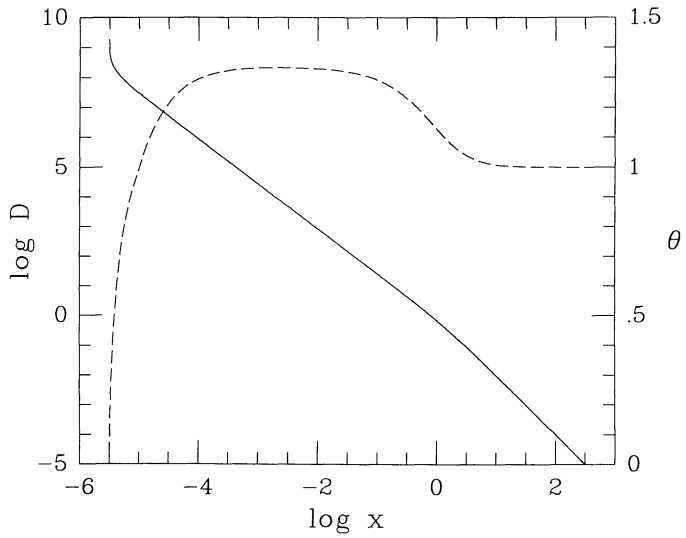

FIG. 4.—Combined self-similar cooling wave and transsonic accretion solution, for $\alpha = \beta = 2$, $\lambda = \frac{1}{2}$. The dimensionless density D (*solid curve, vertical scale on the left*) and temperature θ (*dashed curve, vertical scale on the right*) are plotted against the radius in units of the cooling radius. The sonic radius is at $x = 10^{-5}$.

galaxy M87 in the Virgo cluster. Because of its relative proximity (a distance of 15 Mpc is adopted here) and strong X-ray emission, M87 is the best observed cooling flow and provides the best test of theoretical models. Many groups have previously modeled the X-ray emission around M87, including Binney and Cowie (1981), Fabricant and Gorenstein (1983), Tucker and Rosner (1983), Stewart *et al.* (1984), Bertschinger and Meiksin (1986), and others. All of these previous treatments have assumed steady flow, which as shown in § II, is valid only well interior to the cooling radius. The present treatment relaxes the assumption of steady flow but does not include the effects of star formation or heat conduction considered by previous investigators.

The cooling wave models derived in this paper require power-law approximations to the binding mass profile, cooling function, and initial gas density profile. The binding mass and gas density are obtained from Stewart *et al.* (1984), who combined the available X-ray imaging and spectroscopic data for M87. The gas density follows rather directly from the X-ray surface brightness distribution measured with the *Einstein Observatory* (e.g., Fabricant and Gorenstein 1983). A good fit to the electron density distribution obtained by Stewart *et al.*, valid to within 5% for 2 kpc $< r <$ 200 kpc, is given by (Bertschinger and Meiksin 1986)

$$n_e(r) = 1.46 \times 10^{-2} \frac{(r/30\ \mathrm{kpc})^{-0.8}}{1 + (r/30\ \mathrm{kpc})}\ \mathrm{cm}^{-3}\ . \qquad (4.1)$$

The binding mass profile is considerably more uncertain. In principle, it follows from the density and temperature profiles through the equation of hydrostatic equilibrium, but the distribution of temperature around M87 is not well known. An extensive discussion of this problem is given by Stewart *et al.*, whose results are adopted here. A reasonable fit to their mass distribution, correct to $\sim$15% for 5 kpc $< r <$ 100 kpc, is

$$M_G(r) = 2.4 \times 10^{10} (r/1\ \mathrm{kpc})^{1.3}\ M_\odot\ . \qquad (4.2)$$

The cooling rate is taken to be

$$\mathscr{L} = 1.2 \times 10^{-23} n_e n_\mathrm{H}\ \mathrm{ergs\ cm^{-3}\ s^{-1}}\ , \qquad (4.3)$$

appropriate for a gas of half-solar metal abundances and temperature in the range 0.6–3 $\times 10^7$ K (Gaetz and Salpeter 1983).

Equations (4.1)–(4.3) imply that the dimensionless exponents describing the M87 cooling flow are (see eqs. [2.1], [2.2], and [2.4])

$$\alpha = 1.8\ ,\quad \beta = 1.5\ ,\quad \lambda = 0.0\ , \qquad (4.4)$$

assuming that the cooling radius exceeds 30 kpc. If the cooling flow has an age $10^{10}\tau_{10}$ yr, the cooling radius is (eq. [2.5])

$$R_c = 82\tau_{10}^{\eta}\ \mathrm{kpc}\ ,\quad \eta = 1/2.1 \approx 0.48\ . \qquad (4.5)$$

The propagation speed of the cooling wave is $\dot{R} = 3.8\tau_{10}^{-0.52}$ km s^{-1}, much less than the sound speed at R_c. The square of the cooling wave Mach number is therefore small (eq. [2.15]),

$$\epsilon = 3.4 \times 10^{-5} \tau_{10}^{-1.19}\ , \qquad (4.6)$$

and the separation of the cooling flow into regions of self-similar subsonic flow and steady transsonic flow is well justified.

The cooling wave similarity solution determined by equations (4.4) is gravity-dominated, with $\mu_0 = 1.231$ and $t\dot{m}/m(r = R_c) = 0.382$, yielding the rather high central accretion rate

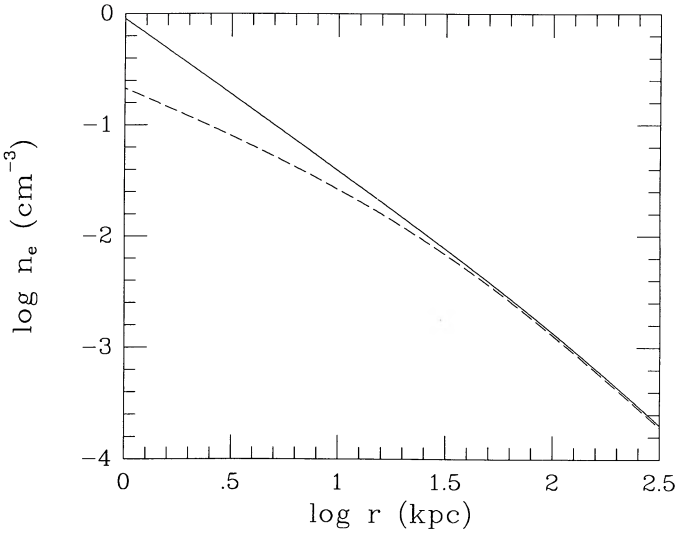

FIG. 5.—Electron density profiles for the cooling flow onto M87. The observationally inferred density profile (from Stewart *et al.* 1984) is given by the dashed curve; the solid curve gives the prediction of the similarity solution matching the observations at large radius. The disagreement at small radius is significant.

(even higher in the past)

$$\dot{m}(r = 0) = 15\tau_{10}^{-0.43}\ M_\odot\ \mathrm{yr}^{-1}\ . \qquad (4.7)$$

The sonic radius occurs inside 1 kpc. The similarity solution does not provide a good fit to the observationally inferred gas distribution. Figure 5, comparing the observed electron density profile (eq. [4.1]) and the profile computed from the similarity solution, illustrates the problem. Beyond the cooling radius, the two profiles agree very well; this agreement has been forced by matching the densities at large radius. Interior to $\sim$20 kpc, however, the density computed from the similarity solution is systematically too high, by an amount almost certainly exceeding the observational uncertainties. It is difficult to quantify this statement because Stewart *et al.* (1984) did not assign errors for their density profile. Figure 6 shows that the temperature profiles agree somewhat better—although there is still a systematic difference between theory and observations, the disagreement is probably smaller than the observational uncertainties.

The discrepancy between the similarity solution and the observations of M87 shows that the time dependence of the outer boundary conditions does not explain the failure of models without heating or star formation found by Stewart *et al.* (1984). Following Takahara and Takahara (1981) and Tucker and Rosner (1983), Bertschinger and Meiksin (1986) suggested that heat conduction might decrease the inflow rate at small radius enough to solve this problem. However, the Fe XVII line emission reported by Canizares, Markert, and Donahue (1988) suggests that heat conduction is not a large factor in the energetics. The explanation favored by many workers is that star formation removes gas from the cooling flow, preventing excessive central X-ray emission.

Star formation is plausible in the context of the cooling wave solutions presented here. Mathews and Bregman (1978), Balbus (1986), and White and Sarazin (1987) show that cooling flows are unstable to short-wavelength, isobaric, comoving thermal instabilities if $\lambda < 2$. For such a perturbation of ampli-

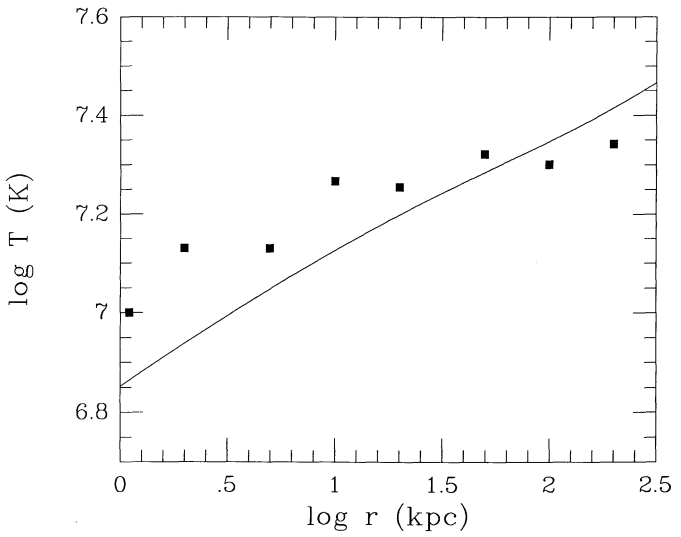

FIG. 6

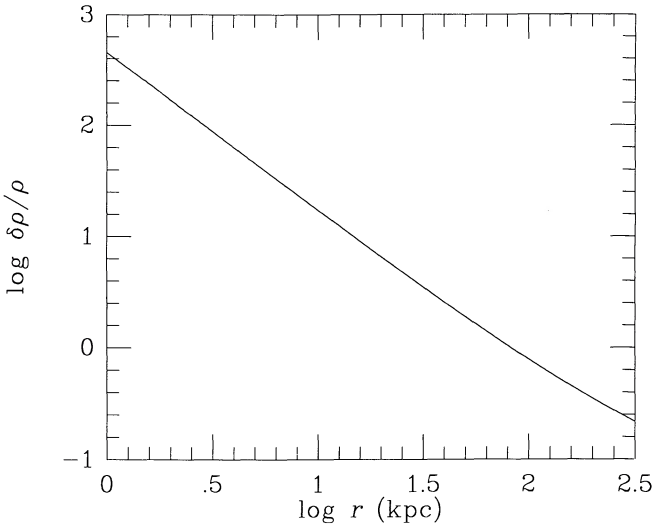

FIG. 7

FIG. 6.—Theoretical (*solid curve*) and observationally inferred (*points*, from Stewart *et al.* 1984) temperature profiles for the M87 cooling flow. Observational errors are difficult to assign, but the observational results are probably consistent with the theoretical model.

FIG. 7.—Linear growth factor, normalized to unity at $r = R_c$, for comoving isobaric density perturbations of the cooling wave solution presented in Figs. 5 and 6.

tude $\delta \equiv \delta\rho/\rho$, the perturbation at r is given up to an arbitrary normalization factor by

$$\ln \delta = \frac{2}{5} \int_r^\infty \left(2 - \frac{d \ln \Lambda}{d \ln T}\right) \frac{\rho^2 \Lambda(T)}{p} \frac{dr}{|v|} . \qquad (4.8)$$

Although equation (4.8) suggests exponential growth, δ grows only as a power of radius because the gas flows in essentially as fast as it cools.

Equation (4.8) is readily evaluated for the similarity solution fit to M87. The result is shown in Figure 7. The normalization has been chosen so that $\delta = 1$ at $r = R_c$. Since the growth is slow for $r \gg R_c$, large preexisting density perturbations must be present if gas is to drop out near R_c. A more conservative view is that $\sim 10\%$ density perturbations are present at R_c due to entropy perturbations produced during cluster virialization or gas injection. These perturbations would become nonlinear within $r \approx 15$ kpc. While the evolution of these perturbations may be complicated by buoyancy (Malagoli, Rosner, and Bodo 1987), it is plausible that once the perturbations become sufficiently nonlinear, dense blobs would cool below X-ray emitting temperatures. Demonstrating this in detail would require multidimensional numerical hydrodynamic simulations. If the gas does begin to drop out near 15 kpc, then the theoretical density profile (Fig. 5) might be brought into satisfactory agreement with observations (Stewart *et al.* 1984).

V. CONCLUSIONS

Time-dependent models of cooling flows can be constructed without resorting to numerical integration of the full partial differential equations of gasdynamics. Such models are self-similar, meaning that there is a unique scale length—the cooling radius, where the cooling time equals the age—which expands as a power-law function of time. Similarity solutions generalize the steady cooling flow solutions considered by previous investigators by incorporating time-dependent effects important in the vicinity of the cooling radius. Self-similar cooling waves present a model for the evolution of the intergalactic medium in clusters of galaxies containing a central dominant galaxy.

The evolution of a cooling flow is self-similar only if the cooling function and the binding mass profile are given by power-law functions, and the gas distribution at large radius is polytropic. Also, the cooling wave must propagate subsonically, and optically thin gas cooling is the only nonadiabatic physical process allowed; otherwise, multiple length scales would exist. Subject to these limitations, there is a three-parameter family of similarity solutions which has been explored in this paper. It has been shown that the similarity solutions can be extended to pass through a sonic point at small radius, by matching the similarity solutions to transsonic cooling accretion solutions.

The self-similar cooling wave model does not provide a good fit to the X-ray emission around M87 at small radius, indicating that time dependence of the outer boundary conditions alone does not explain the discrepancy between observations and steady state models without star formation or heating. Nevertheless, the cooling wave model is instructive. From the similarity solutions it is clear that time-dependent effects are small well inside of the cooling radius, but that they are important near R_c. Time dependence causes a steepening of the X-ray brightness profile (since it steepens the gas density profile) even if the initial density and pressure profiles are pure power-laws of radius.

A local linear stability analysis has shown that isobaric perturbations may grow enough for gas to drop out of the M87 cooling flow at small radius, suggesting that the neglect of star formation may account for the disagreement with observations. However, perturbations do not grow much beyond the cooling radius, so that the amplitude of density perturbations outside of the cooling flow must be large if gas is to drop out before reaching R_c. Finally, the results imply that, at least in the case of M87 and even neglecting cluster dynamical evolution, cooling flows should have been more vigorous in the past.

I would like to thank Marc Davis, Chris McKee, and Avery Meiksin for helpful comments. Support for this work was provided by the Miller Institute for Basic Research in Science at the University of California at Berkeley and by NASA Astrophysics Theory grant NAGW-1320.

APPENDIX A

JUSTIFICATION FOR NEGLECTING ACCELERATION TERMS

The similarity solutions of § II are derived under the assumption that the time-dependent acceleration terms in the momentum equation (2.13) can be neglected outside the sonic radius and interior to the rarefaction wave. This assumption appears plausible since the flow is highly subsonic, but a rigorous demonstration of its validity is presented here. The demonstration consists of two parts: first, showing that the solution obtained is self-consistent, in that the acceleration terms are indeed small out to the rarefaction wave; and second, showing that in the particular case $\alpha = \beta = 1$, the solution agrees with that of Chevalier (1987), who included the acceleration terms in a fully self-similar solution.

A rarefaction wave travels outward through the gas at the local sound speed, $dR_s/dt = v + (\gamma p/\rho)^{1/2}$. To lowest order in ϵ (the square of the cooling Mach number; see eq. [2.15]),

$$R_s(t) = \left(\frac{\beta - \alpha + 2}{2}\right)\left[\frac{\gamma p_0(R_s)}{\rho_0(R_s)}\right]^{1/2} t \,. \tag{A1}$$

For $\epsilon \ll 1$, the acceleration terms in equation (2.13) are negligible near the cooling wave, $x \sim 1$. But these terms are clearly important at the rarefaction wave, which is a weak discontinuity where the fluid variables have cusps (Chevalier 1987). With the neglect of these terms, a similarity solution can be found, but it is not valid at the rarefaction wave. The question addressed here is whether the solution is therefore invalid interior to the rarefaction wave.

For $x = r/R_c \gtrsim 1$, the ratio of the acceleration terms to the gravitational term in equation (2.13) is monotonic in radius. Since the ratio is small at $x = 1$, self-consistency is ensured, provided that the ratio is also small at $x = x_s(t) = R_s(t)/R_c(t)$. The ratio of the acceleration to gravity terms at $x = x_s$ is

$$\frac{\gamma}{\beta}\left[\frac{\eta(\beta - \alpha + 2)}{2}\right]^2 W_s\left[(1 + W)\frac{d\ln W}{d\ln x} + W + \frac{1}{\eta}\right]_s , \tag{A2}$$

where the subscript indicates that the quantity is to be evaluated at x_s. It is assumed that $0 < \eta(\beta - \alpha + 2)/2 \leq 1$. From equation (2.24), for $\epsilon \ll 1$ and $x_s \propto \epsilon^{-1/(\beta-\alpha+2)} \gg 1$,

$$W_s \approx (\eta E_0)^{-1/e_0}\left[\frac{\eta(\beta - \alpha + 2)}{2}\right]^{-2/e_0\eta(\beta-\alpha+2)} \epsilon^{1/e_0\eta(\beta-\alpha+2)} \ll 1 \,. \tag{A3}$$

Since $W_s \ll 1$ and $d\ln W/d\ln x \approx -1/(\eta e_0)$, it is clear from equation (A2) that for $\epsilon \ll 1$ the acceleration terms are negligible compared to the other terms in equation (2.13) between R_c and R_s. This result is not surprising; it simply reflects the extreme weakness of the rarefaction wave for $\epsilon \ll 1$. Only in the immediate vicinity of the rarefaction wave are the acceleration terms important.

The second part of the demonstration is to show that even though the acceleration terms are important right at the rarefaction wave, this does not affect the validity of the similarity solution downstream of the wave. The proof consists of comparing the fully self-similar solution found by Chevalier (1987) for the case $\alpha = \beta = 1$ with the piecewise self-similar solution found here. Chevalier's restriction to cases for which $\epsilon =$ constant ensures that the flow is fully self-similar even including the acceleration terms. For $\epsilon =$ constant $\ll 1$ the solution found here neglecting the acceleration terms should agree Chevalier's solution between the cooling and rarefaction waves (his region III).

For $\alpha = \beta = \eta = 1$, the solution found by Chevalier (1987) for $R_c \ll r \ll R_s$ yields (his eq. [21])

$$\frac{v}{c_0} = -\frac{4}{11}a \,, \qquad \frac{p}{\rho c_0^2} = 1 - \frac{2a}{11\eta'} \,, \tag{A4}$$

where $c_0 = (B/A)^{1/2}$ is the initial isothermal sound speed, a is a small parameter proportional to the cooling wave Mach number, and $\eta' = r/(c_0 t)$. To first order in ϵ the density equals its initial value $\rho_0(r)$. Using equations (4) and (8) of Chevalier and equations (2.1), (2.6), and (2.15) in the present paper, one finds

$$a = (\gamma\epsilon)^{1/2}/(\gamma - 1) \,, \qquad \eta' = (\gamma\epsilon)^{1/2} \,, \tag{A5}$$

with $\gamma = 5/3$.

Now equations (A4) may be compared with the results obtained in this paper. For $\alpha = \beta = \eta = 1$, equation (B1) of Appendix B gives $\delta = \chi = 2$; from equations (B2) and (B4) it follows that $e_0 = 1$, $\zeta = -1$, $Q_1 = -\frac{1}{2}$, and $E_0 = 11/6$. By assumption, $x \gg 1$, so that $W \ll 1$. Then equation (2.24) yields

$$-\frac{vt}{R_c} = xW = \frac{1}{E_0} = \frac{6}{11} \,, \qquad \frac{p}{\rho c_0^2} = Q = 1 + Q_1 W = 1 - \frac{1}{2}W \,. \tag{A6}$$

Using equations (A5) to convert to Chevalier's units, these results agree exactly with equations (A4). Therefore, even though the rarefaction wave is neglected in the present work, the flow interior to it is followed correctly provided that the flow beyond the cooling wave is extremely subsonic.

APPENDIX B

ASYMPTOTIC FORM OF THE SIMILARITY SOLUTIONS FOR LARGE x

Since the cooling wave similarity solutions derived in § II are integrated numerically inward from $x \gg 1$, a power series expansion of the solutions for large x is necessary to provide starting values. Equations (2.24) give the form of the series expansions satisfying the outer boundary conditions equations (2.23). This Appendix provides expressions for the power series exponents and coefficients satisfying the nondimensional fluid equations (2.18)–(2.21).

Substitution of the power series expansions equations (2.24) into the fluid equations provides a set of equations for the series coefficients and exponents, which must be satisfied order by order in the expansion in powers of W. These equations are tedious and are not reproduced here, although the results are used below. For convenience, the following frequently occurring groups of constants are defined:

$$\delta \equiv \eta(3-\alpha)\,, \qquad \zeta \equiv 1-\delta e_0\,, \qquad \chi \equiv (\gamma-1)\delta+\eta(\gamma\alpha-\beta)\,. \tag{B1}$$

It will be assumed throughout that $\alpha < 3$ so that the gas mass converges as $x \to 0$, and that $\gamma\alpha > \beta$, so that the initial equilibrium state is convectively stable. Since only expanding waves are under consideration, $\eta > 0$, and therefore $\delta > 0$ and $\chi > 0$.

The lowest order terms in the expansion of equation (2.18) yield the results

$$q_1 = 1\,, \qquad Q_1 = \frac{\zeta}{1+e_0\eta\beta}\,. \tag{B2}$$

Equation (2.19) implies $e_0 \geq 1$; thus, there are two cases to be considered: $e_0 = 1$ and $e_0 > 1$. In both cases, the exponents of W in the series for Q and E are simply related:

$$q_2 = 1+e_1\,, \qquad q_3 = 1+e_2\,. \tag{B3}$$

Consider first the case $e_0 = 1$. Equation (B2) gives Q_1 directly, while the lowest order terms in the expansion of equation (2.19) give E_0:

$$E_0 = \frac{\chi-(Q_1+\gamma-1)}{\eta}\,. \tag{B4}$$

The case $e_0 = 1$ applies provided this expression yields $E_0 > 0$. The next order in the expansion yields a quadratic for e_1:

$$\gamma e_1^2+[1-Q_1-\eta E_0+(Q_1+\gamma-1)(1+\eta\beta)]e_1-(1+\eta\beta)\eta E_0 = 0; \tag{B5}$$

for $E_0 > 0$ there is exactly one positive root.

The case $e_0 = 1$ is subdivided into three different possibilities: $e_1 < \frac{1}{2}$, $\frac{1}{2} < e_1 < 1$, and $e_1 > 1$. (The cases $e_1 = \frac{1}{2}$ and $e_1 = 1$ may be obtained by taking limits.) In the first two cases, $e_0 = 1$ and $e_1 < 1$, E_1 is arbitrary (an eigenvalue). Given E_1, Q_2 follows:

$$Q_2 = \frac{-(\delta+\eta\beta Q_1)e_1}{1+e_1+\eta\beta}\,E_1\,. \tag{B6}$$

If $e_0 = 1$ and $e_1 < \frac{1}{2}$, then

$$e_2 = 2e_1\,, \tag{B7}$$

and E_2 and Q_3 follow from solving the pair of linear equations

$$\begin{aligned}(\delta+\eta\beta Q_1)e_2E_2+(1+e_2+\eta\beta)Q_3 &= [(\delta+\eta\beta Q_1)E_1-\eta\beta Q_2]e_1E_1\,,\\ [(1+e_2)\eta E_0-\chi e_2]E_2+(1+e_2)Q_3 &= -\chi e_1E_1^2\,.\end{aligned} \tag{B8}$$

Once E_1 is specified, E_2 and Q_3 follow simply.

If $e_0 = 1$ and $\frac{1}{2} < e_1 < 1$, then

$$e_2 = 1\,, \tag{B9}$$

with E_2 and Q_3 following from solving

$$\begin{aligned}(\delta+\eta\beta Q_1)E_2+(2+\eta\beta)Q_3 &= -\zeta(\delta+\eta\beta Q_1+1-Q_1)\,,\\ (2\eta E_0-\chi)E_2+2Q_3 &= \zeta(Q_1+\gamma-1)+Q_1(Q_1-1)+(1-\lambda)Q_1\eta E_0\,.\end{aligned} \tag{B10}$$

When $e_0 = 1$ and equation (B5) gives $e_1 > 1$, the power series for E and Q must be reordered, because the series contain terms $\propto W_1$. To maintain a proper ordering, one must have $e_2 > e_1$, so in this case one sets $e_1 = 1$, while e_2 is set equal to the positive root

of equation (B5) (formerly e_1). Now E_1 and Q_2 are fixed as the solution of equations (B10) (with $E_2 \to E_1$ and $Q_3 \to Q_2$), while E_2 is an arbitrary eigenvalue, with Q_3 following from equation (B6), with $e_1 \to e_2$ and $E_1 \to E_2$.

If equation (B4) gives $E_0 \le 0$, the assumption $e_0 = 1$ is incorrect, since the density must be positive. In this case e_0 is the positive root of the quadratic

$$\eta\beta\chi e_0^2 + \gamma\eta(3 - \beta)e_0 - \gamma = 0 . \tag{B11}$$

It is straightforward to show that there is a root $e_0 > 1$ for $\chi > 0$ if and only if equation (B4) gives $E_0 < 0$. Now E_0 is an arbitrary eigenvalue.

As in the earlier case $e_0 = 1$, the case $e_0 > 1$ is divided three ways: $e_0 < 3/2$, $3/2 < e_0 < 2$, and $e_0 > 2$. In the first two cases, $1 < e_0 < 2$, one obtains

$$e_1 = e_0 - 1 . \tag{B12}$$

Now E_1 and Q_2 follow from solving the pair of linear equations

$$(\delta + \eta\beta Q_1)e_1 E_1 + (1 + e_1 + e_0\eta\beta)Q_2 = 0 , \qquad \chi e_1 E_1 - (1 + e_1)Q_2 = e_0\eta E_0 . \tag{B13}$$

If $1 < e_0 < 3/2$ ($e_1 < 1/2$), then $e_2 = 2e_1$ (see eq. [B7]) and E_2 and Q_3 follow from

$$\begin{aligned}(\delta + \eta\beta Q_1)e_2 E_2 + (1 + e_2 + e_0\eta\beta)Q_3 &= [(\delta + \eta\beta Q_1)E_1 - \eta\beta Q_2]e_1 E_1 , \\ \chi e_2 E_2 - (1 + e_2)Q_3 &= (e_0 + e_1)\eta E_0 E_1 + \chi e_1 E_1^2 .\end{aligned} \tag{B14}$$

Once E_0 is specified, E_1, E_2, Q_2, and Q_3 follow.

If $3/2 < e_0 < 2$ ($1/2 < e_1 < 1$), then $e_2 = 1$ (see eq. [B9]), with E_2 and Q_3 following from the solution to

$$\begin{aligned}(\delta + \eta\beta Q_1)e_2 E_2 + (1 + e_2 + e_0\eta\beta)Q_3 &= -\zeta(\delta + \eta\beta Q_1 + 1 - Q_1) , \\ \chi e_2 E_2 - (1 + e_2)Q_3 &= -\zeta\chi + Q_1(1 - Q_1) .\end{aligned} \tag{B15}$$

Finally, when $e_0 > 2$, equation (B12) would give $e > 1$; as before, there are terms $\propto W^1$ in the series. Thus, a reordering is again necessary. The correct solution is obtained by setting $e_1 = 1$ and $e_2 = e_0 - 1$. The series coefficients E_1, E_2, Q_2, and Q_3 follow from solution of equations (B13) and (B15), after exchanging the pairs (e_1, e_2), (E_1, E_2), and (Q_2, Q_3).

REFERENCES

Balbus, S. A. 1986, *Ap. J. (Letters)*, **303**, L79.
Bertschinger, E. 1986, *Ap. J.*, **304**, 154.
———. 1988, in *Cooling Flows in Clusters and Galaxies*, ed. A. C. Fabian (Dordrecht: Kluwer Academic Press), p. 337.
Bertschinger, E., and Meiksin, A. 1986, *Ap. J. (Letters)*, **306**, L1.
Binney, J., and Cowie, L. L. 1981, *Ap. J.*, **247**, 464.
Bondi, H. 1952, *M.N.R.A.S.*, **112**, 195.
Bregman, J. N., and David, L. P. 1988, *Ap. J.*, **326**, 639.
Canizares, C. R., Markert, T. H., and Donahue, M. E. 1988, in *Cooling Flows in Clusters and Galaxies*, ed. A. C. Fabian (Dordrecht: Kluwer Academic Press), p. 63.
Chevalier, R. A. 1987, *Ap. J.*, **318**, 66.
Chevalier, R. A., and Imamura, J. N. 1982, *Ap. J.*, **261**, 543.
Cowie, L. L., and Binney, J. 1977, *Ap. J.*, **215**, 723.
Cowie, L. L., Fabian, A. C., and Nulsen, P. E. J. 1980, *M.N.R.A.S.*, **191**, 399.
Cowie, L. L., and Perrenod, S. C. 1978, *Ap. J.*, **219**, 354.
Fabian, A. C., Hu, E. M., Cowie, L. L., and Grindlay, J. 1981, *Ap. J.*, **248**, 47.
Fabian, A. C., and Nulsen, P. E. J. 1977, *M.N.R.A.S.*, **180**, 479.
———. 1979, *M.N.R.A.S.*, **186**, 783.
Fabian, A. C., Nulsen, P. E. J., and Canizares, C. R. 1982, *M.N.R.A.S.*, **201**, 933.
———. 1984, *Nature*, **310**, 733.
Fabian, A. C., *et al.* 1985, *M.N.R.A.S.*, **216**, 923.
Fabricant, D., and Gorenstein, P. 1983, *Ap. J.*, **267**, 535.
Friaca, A. C. S. 1986, *Astr. Ap.*, **164**, 6.
Gaetz, T. J., and Salpeter, E. E. 1983, *Ap. J. Suppl.*, **52**, 155.
Gull, S. F., and Northover, K. J. E. 1975, *M.N.R.A.S.*, **173**, 585.
Jones, C., and Forman, W. 1984, *Ap. J.*, **276**, 38.
Lea, S. M. 1976, *Ap. J.*, **203**, 569.
Malagoli, A., Rosner, R., and Bodo, G. 1987, *Ap. J.*, **319**, 632.
Mathews, W. G., and Bregman, J. N. 1978, *Ap. J.*, **224**, 308.
Meiksin, A. 1988, in *Cooling Flows in Clusters and Galaxies*, ed. A. C. Fabian (Dordrecht: Kluwer Academic Press), p. 47.
Nulsen, P. E. J., Stewart, G. C., and Fabian, A. C. 1984, *M.N.R.A.S.*, **208**, 185.
Nulsen, P. E. J., Stewart, G. C., Fabian, A. C., Mushotzky, R. F., Holt, S. S., Ku, W. H.-M., and Malin, D. F. 1982, *M.N.R.A.S.*, **199**, 1089.
Perrenod, S. C. 1978, *Ap. J.*, **226**, 566.
Sarazin, C. L. 1986, *Rev. Mod. Phys.*, **58**, 1.
Sedov, L. I. 1959, *Similarity and Dimensional Methods in Mechanics* (New York: Academic).
Shu, F. H. 1977, *Ap. J.*, **214**, 488.
Silk, J. 1976, *Ap. J.*, **208**, 646.
Silk, J., Djorgovski, S., Wyse, R. F. G., and Bruzual, G. 1986, *Ap. J.*, **307**, 415.
Stewart, G. C., Canizares, C. R., Fabian, A. C., and Nulsen, P. E. J. 1984, *Ap. J.*, **278**, 536.
Takahara, F., Ikeuchi, S., Shibazaki, N., and Hoshi, R. 1976, *Progr. Theor. Phys.*, **56**, 1093.
Takahara, M., and Takahara, F. 1981, *Progr. Theor. Phys. (Letters)*, **65**, 369.
Tucker, W. H., and Rosner, R. 1983, *Ap. J.*, **267**, 547.
White, R. E., and Sarazin, C. L. 1986, *Ap. J.*, **318**, 612.

EDMUND BERTSCHINGER: Department of Physics, MIT, Room 6-207, Cambridge, MA 02139